

Supplemental Information

A pseudo-first-order kinetic signature for parallel pathways: conformational selection *and* induced fit.

Eric A. Galburt and Jayan Rammohan

To whom correspondence should be addressed. Tel: (314)362-5201 Email: egalburt@biochem.wustl.edu

Department of Biochemistry and Molecular Biophysics, Washington University School of Medicine, St. Louis, MO 63110, USA

Analytical expression for $\lambda_3 (k_{\text{obs},3})$:

$$\begin{aligned}
 & -(((k_{12} + k_{34} + k_{21} + k_{31} + k_{42} + k_{43} + L*k_{13} + L*k_{24})*(k_{12}*k_{34} + k_{12}*k_{31} + k_{12}*k_{42} + k_{12}*k_{43} + k_{34}*k_{21} + k_{34}*k_{42} + k_{21}*k_{31} + k_{21}*k_{42} + k_{21}*k_{43} + k_{31}*k_{42} + k_{31}*k_{43} + L*k_{12}*k_{24} + L*k_{13}*k_{34} + L*k_{24}*k_{34} + L*k_{13}*k_{21} + L*k_{13}*k_{42} + L*k_{24}*k_{31} + L*k_{13}*k_{43} + L*k_{24}*k_{43} + L^2*k_{13}*k_{24})))/6 \\
 & -(k_{12} + k_{34} + k_{21} + k_{31} + k_{42} + k_{43} + L*k_{13} + L*k_{24})^{3/27} + (((k_{12} + k_{34} + k_{21} + k_{31} + k_{42} + k_{43} + L*k_{13} + L*k_{24})^{3/27} - ((k_{12} + k_{34} + k_{21} + k_{31} + k_{42} + k_{43} + L*k_{13} + L*k_{24})*((k_{12}*k_{34} + k_{12}*k_{31} + k_{12}*k_{42} + k_{12}*k_{43} + k_{34}*k_{21} + k_{34}*k_{42} + k_{21}*k_{31} + k_{21}*k_{42} + k_{21}*k_{43} + k_{31}*k_{42} + k_{31}*k_{43} + L*k_{12}*k_{24} + L*k_{13}*k_{34} + L*k_{24}*k_{34} + L*k_{13}*k_{21} + L*k_{13}*k_{42} + L*k_{24}*k_{31} + L*k_{13}*k_{43} + L*k_{24}*k_{43} + L^2*k_{13}*k_{24}))/6 + (k_{12}*k_{34}*k_{42})/2 + (k_{12}*k_{31}*k_{42})/2 + (k_{12}*k_{31}*k_{43})/2 + (k_{34}*k_{21}*k_{42})/2 + (k_{21}*k_{31}*k_{42})/2 + (k_{21}*k_{31}*k_{43})/2 + (L^2*k_{13}*k_{24}*k_{34})/2 + (L*k_{12}*k_{24}*k_{34})/2 + (L*k_{12}*k_{24}*k_{31})/2 + (L*k_{13}*k_{34}*k_{21})/2 + (L*k_{12}*k_{24}*k_{43})/2 + (L*k_{13}*k_{34}*k_{42})/2 + (L*k_{13}*k_{21}*k_{42})/2 + (L*k_{13}*k_{21}*k_{43})/2 + (L*k_{24}*k_{31}*k_{43})/2)^2 + ((k_{12}*k_{34})/3 + (k_{12}*k_{31})/3 + (k_{12}*k_{42})/3 + (k_{12}*k_{43})/3 + (k_{34}*k_{21})/3 + (k_{34}*k_{42})/3 + (k_{21}*k_{31})/3 + (k_{21}*k_{42})/3 + (k_{21}*k_{43})/3 + (k_{31}*k_{42})/3 + (k_{31}*k_{43})/3 - (k_{12} + k_{34} + k_{21} + k_{31} + k_{42} + k_{43} + L*k_{13} + L*k_{24})^{2/9} + (L*k_{12}*k_{24})/3 + (L*k_{13}*k_{34})/3 + (L*k_{24}*k_{34})/3 + (L*k_{13}*k_{21})/3 + (L*k_{13}*k_{42})/3 + (L*k_{24}*k_{31})/3 + (L*k_{13}*k_{43})/3 + (L^2*k_{13}*k_{24}))/3)^{(1/2)} - (k_{12}*k_{34}*k_{42})/2 - (k_{12}*k_{31}*k_{42})/2 - (k_{12}*k_{31}*k_{43})/2 - (k_{34}*k_{21}*k_{42})/2 - (k_{21}*k_{31}*k_{43})/2 - (L^2*k_{13}*k_{24}*k_{34})/2 - (L^2*k_{13}*k_{24}*k_{43})/2 - (L*k_{12}*k_{24}*k_{34})/2 - (L*k_{12}*k_{24}*k_{31})/2 - (L*k_{13}*k_{34}*k_{21})/2 - (L*k_{12}*k_{24}*k_{43})/2 - (L*k_{13}*k_{34}*k_{42})/2 - (L*k_{13}*k_{21}*k_{42})/2 - (L*k_{24}*k_{31}*k_{43})/2 - (L*k_{24}*k_{31})^{(1/3)} - k_{34}/3 - k_{21}/3 - k_{31}/3 - k_{42}/3 - k_{43}/3 - (L*k_{13})/3 - (L*k_{24})/3 - ((k_{12}*k_{34})/3 + (k_{12}*k_{31})/3 + (k_{12}*k_{42})/3 + (k_{12}*k_{43})/3 + (k_{34}*k_{21})/3 + (k_{34}*k_{42})/3 + (k_{21}*k_{31})/3 + (k_{21}*k_{42})/3 + (k_{21}*k_{43})/3 + (k_{31}*k_{42})/3 - (k_{12} + k_{34} + k_{21} + k_{31} + k_{42} + k_{43} + L*k_{13} + L*k_{24})^{2/9} + (L*k_{12}*k_{24})/3 + (L*k_{13}*k_{34})/3 + (L*k_{24}*k_{34})/3 + (L*k_{13}*k_{21})/3 + (L*k_{13}*k_{42})/3 + (L*k_{24}*k_{31})/3 + (L*k_{13}*k_{43})/3 + (L^2*k_{13}*k_{24}))/3)^{(1/3)} / (((k_{12} + k_{34} + k_{21} + k_{31} + k_{42} + k_{43} + L*k_{13} + L*k_{24})*(k_{12}*k_{34} + k_{12}*k_{31} + k_{12}*k_{42} + k_{12}*k_{43} + k_{34}*k_{21} + k_{34}*k_{42} + k_{21}*k_{31} + k_{21}*k_{42} + k_{21}*k_{43} + k_{31}*k_{42} + k_{31}*k_{43} + L*k_{12}*k_{24} + L*k_{13}*k_{34} + L*k_{24}*k_{34} + L*k_{13}*k_{21} + L*k_{13}*k_{42} + L*k_{24}*k_{31} + L*k_{13}*k_{43} + L*k_{24}*k_{34} + L^2*k_{13}*k_{24}))/6 - (k_{12} + k_{34} + k_{21} + k_{31} + k_{42} + k_{43} + L*k_{13} + L*k_{24})^{3/27} - ((k_{12} + k_{34} + k_{21} + k_{31} + k_{42} + k_{43} + L*k_{13} + L*k_{24})*(k_{12}*k_{34} + k_{12}*k_{31} + k_{12}*k_{42} + k_{12}*k_{43} + k_{34}*k_{21} + k_{34}*k_{42} + k_{21}*k_{31} + k_{21}*k_{42} + k_{21}*k_{43} + k_{31}*k_{42} + k_{31}*k_{43} + L*k_{12}*k_{24} + L*k_{13}*k_{34} + L*k_{24}*k_{34} + L*k_{13}*k_{21} + L*k_{13}*k_{42} + L*k_{24}*k_{31} + L*k_{13}*k_{43} + L*k_{24}*k_{34} + L^2*k_{13}*k_{24}))/6 + (k_{12}*k_{34}*k_{42})/2 + (k_{12}*k_{31}*k_{42})/2 + (k_{12}*k_{31}*k_{43})/2 + (k_{34}*k_{21}*k_{42})/2 + (k_{21}*k_{31}*k_{42})/2 + (k_{21}*k_{31}*k_{43})/2 + (L^2*k_{13}*k_{24}*k_{34})/2 + (L*k_{12}*k_{24}*k_{34})/2 + (L*k_{12}*k_{24}*k_{31})/2 + (L*k_{13}*k_{34}*k_{21})/2 + (L*k_{12}*k_{24}*k_{43})/2 + (L*k_{13}*k_{34}*k_{42})/2 + (L*k_{13}*k_{21}*k_{42})/2 + (L*k_{24}*k_{31}*k_{43})/2)^2 + ((k_{12}*k_{34})/3 + (k_{12}*k_{31})/3 + (k_{12}*k_{42})/3 + (k_{12}*k_{43})/3 + (k_{34}*k_{21})/3 + (k_{34}*k_{42})/3 + (k_{21}*k_{31})/3 + (k_{21}*k_{42})/3 + (k_{21}*k_{43})/3 + (k_{31}*k_{42})/3 + (k_{31}*k_{43})/3 - (k_{12} + k_{34} + k_{21} + k_{31} + k_{42} + k_{43} + L*k_{13} + L*k_{24})^{2/9} + (L*k_{12}*k_{24})/3 + (L*k_{13}*k_{34})/3 + (L*k_{24}*k_{34})/3 + (L*k_{13}*k_{21})/3 + (L*k_{13}*k_{42})/3 + (L*k_{24}*k_{31})/3 + (L*k_{13}*k_{43})/3 + (L^2*k_{13}*k_{24}))/3)^{(1/2)} - (k_{12}*k_{34}*k_{42})/2 - (k_{12}*k_{31}*k_{42})/2 - (k_{12}*k_{31}*k_{43})/2 - (k_{34}*k_{21}*k_{42})/2 - (k_{21}*k_{31}*k_{43})/2 - (L^2*k_{13}*k_{24}*k_{34})/2 - (L*k_{12}*k_{24}*k_{34})/2 - (L*k_{12}*k_{24}*k_{31})/2 - (L*k_{13}*k_{34}*k_{21})/2 - (L*k_{12}*k_{24}*k_{43})/2 - (L*k_{13}*k_{34}*k_{42})/2 - (L*k_{13}*k_{21}*k_{42})/2 - (L*k_{24}*k_{31}*k_{43})/2 - (L*k_{24}*k_{31})^{(1/3)} - k_{12}/3)
 \end{aligned}$$

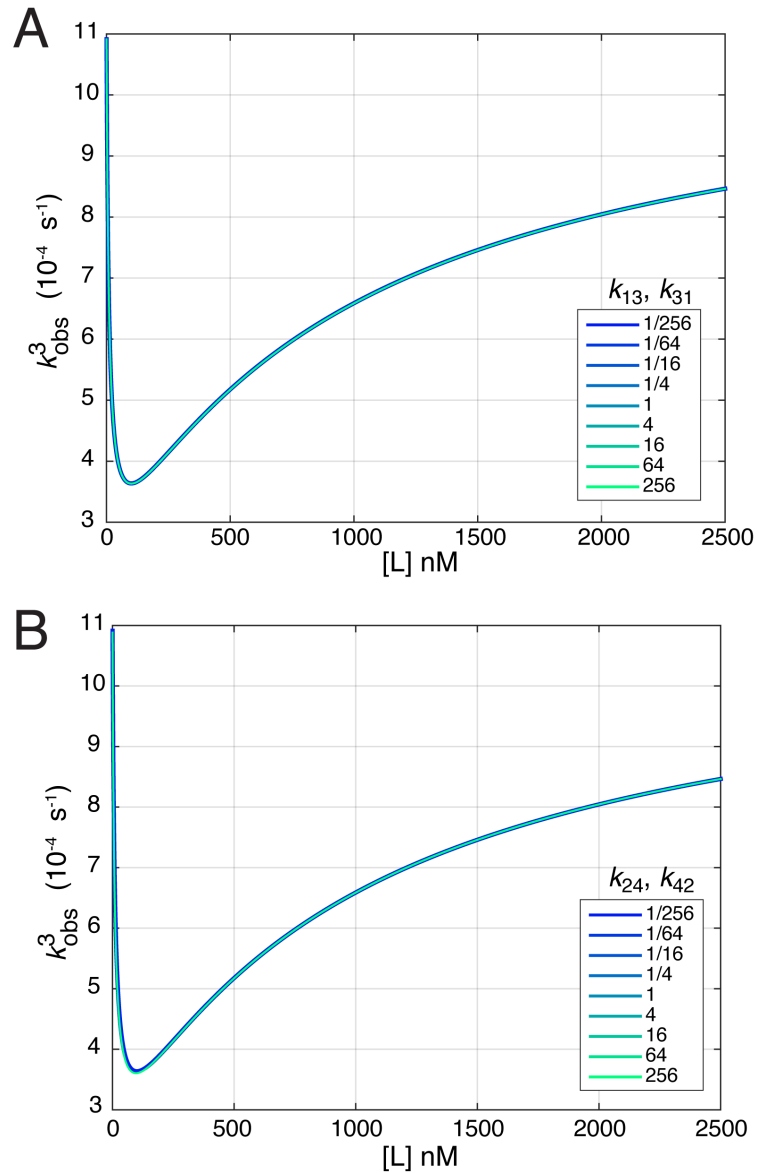
Analytical expression for $d\lambda_3/d[L]$ ($dk_{\text{obs},3}/d[L]$):

$$\begin{aligned}
& k_{21} + k_{31} + k_{42} + k_{43} + L*k_{13} + L*k_{24})*(k_{12}*k_{34} + k_{12}*k_{31} + k_{12}*k_{42} + k_{12}*k_{43} + k_{34}*k_{21} + \\
& k_{34}*k_{42} + k_{21}*k_{31} + k_{21}*k_{42} + k_{21}*k_{43} + k_{31}*k_{42} + k_{31}*k_{43} + L*k_{12}*k_{24} + L*k_{13}*k_{34} + \\
& L*k_{24}*k_{34} + L*k_{13}*k_{21} + L*k_{13}*k_{42} + L*k_{24}*k_{31} + L*k_{13}*k_{43} + L*k_{24}*k_{43} + L^2*k_{13}*k_{24})/6 + \\
& (k_{12}*k_{34}*k_{42})/2 + (k_{12}*k_{31}*k_{42})/2 + (k_{12}*k_{31}*k_{43})/2 + (k_{34}*k_{21}*k_{42})/2 + (k_{21}*k_{31}*k_{42})/2 + \\
& (k_{21}*k_{31}*k_{43})/2 + (L^2*k_{13}*k_{24}*k_{34})/2 + (L^2*k_{13}*k_{24}*k_{43})/2 + (L*k_{12}*k_{24}*k_{34})/2 + \\
& (L*k_{12}*k_{24}*k_{31})/2 + (L*k_{13}*k_{34}*k_{21})/2 + (L*k_{12}*k_{24}*k_{43})/2 + (L*k_{13}*k_{34}*k_{42})/2 + \\
& (L*k_{13}*k_{21}*k_{42})/2 + (L*k_{13}*k_{21}*k_{43})/2 + (L*k_{24}*k_{31}*k_{43})/2)^2 + ((k_{12}*k_{34})/3 + (k_{12}*k_{31})/3 + \\
& (k_{12}*k_{42})/3 + (k_{12}*k_{43})/3 + (k_{34}*k_{21})/3 + (k_{34}*k_{42})/3 + (k_{21}*k_{31})/3 + (k_{21}*k_{42})/3 + (k_{21}*k_{43})/3 + \\
& (k_{31}*k_{42})/3 + (k_{31}*k_{43})/3 - (k_{12} + k_{34} + k_{21} + k_{31} + k_{42} + k_{43} + L*k_{13} + L*k_{24})^{2/9} + (L*k_{12}*k_{24})/ \\
& 3 + (L*k_{13}*k_{34})/3 + (L*k_{24}*k_{34})/3 + (L*k_{13}*k_{21})/3 + (L*k_{13}*k_{42})/3 + (L*k_{24}*k_{31})/3 + \\
& (L*k_{13}*k_{43})/3 + (L*k_{24}*k_{43})/3 + (L^2*k_{13}*k_{24})/3)^3)^{(1/2)} - ((k_{12} + k_{34} + k_{21} + k_{31} + k_{42} + k_{43} + \\
& L*k_{13} + L*k_{24})*(k_{12}*k_{24} + k_{13}*k_{34} + k_{24}*k_{34} + k_{13}*k_{21} + k_{13}*k_{42} + k_{24}*k_{31} + k_{13}*k_{43} + \\
& k_{24}*k_{43} + 2*L*k_{13}*k_{24})/6 + (k_{12}*k_{24}*k_{34})/2 + (k_{12}*k_{24}*k_{31})/2 + (k_{13}*k_{34}*k_{21})/2 + \\
& (k_{12}*k_{24}*k_{43})/2 + (k_{13}*k_{34}*k_{42})/2 + (k_{13}*k_{21}*k_{42})/2 + (k_{24}*k_{31}*k_{43})/2 + \\
& L*k_{13}*k_{24}*k_{34} + L*k_{13}*k_{24}*k_{43})*((k_{12}*k_{34})/3 + (k_{12}*k_{31})/3 + (k_{12}*k_{42})/3 + (k_{12}*k_{43})/3 + \\
& (k_{34}*k_{21})/3 + (k_{34}*k_{42})/3 + (k_{21}*k_{42})/3 + (k_{21}*k_{43})/3 + (k_{31}*k_{42})/3 + (k_{31}*k_{43})/3 - \\
& (k_{12} + k_{34} + k_{21} + k_{31} + k_{42} + k_{43} + L*k_{13} + L*k_{24})^{2/9} + (L*k_{12}*k_{24})/3 + (L*k_{13}*k_{34})/3 + \\
& (L*k_{24}*k_{34})/3 + (L*k_{13}*k_{21})/3 + (L*k_{13}*k_{42})/3 + (L*k_{24}*k_{31})/3 + (L*k_{13}*k_{43})/3 + (L*k_{24}*k_{43})/3 + \\
& (L^2*k_{13}*k_{24})/3)/(3*((k_{12} + k_{34} + k_{21} + k_{31} + k_{42} + k_{43} + L*k_{13} + L*k_{24})*(k_{12}*k_{34} + k_{12}*k_{31} + \\
& k_{12}*k_{42} + k_{12}*k_{43} + k_{34}*k_{21} + k_{34}*k_{42} + k_{21}*k_{31} + k_{21}*k_{42} + k_{21}*k_{43} + k_{31}*k_{42} + k_{31}*k_{43} + \\
& L*k_{12}*k_{24} + L*k_{13}*k_{34} + L*k_{24}*k_{34} + L*k_{13}*k_{21} + L*k_{13}*k_{42} + L*k_{24}*k_{31} + L*k_{13}*k_{43} + \\
& L*k_{24}*k_{43} + L^2*k_{13}*k_{24})/6 - (k_{12} + k_{34} + k_{21} + k_{31} + k_{42} + k_{43} + L*k_{13} + L*k_{24})^{3/27} + ((k_{12} + \\
& k_{34} + k_{21} + k_{31} + k_{42} + k_{43} + L*k_{13} + L*k_{24})^{3/27} - ((k_{12} + k_{34} + k_{21} + k_{31} + k_{42} + k_{43} + L*k_{13} + \\
& L*k_{24})*(k_{12}*k_{34} + k_{12}*k_{31} + k_{12}*k_{42} + k_{12}*k_{43} + k_{34}*k_{21} + k_{34}*k_{42} + k_{21}*k_{31} + k_{21}*k_{42} + \\
& k_{21}*k_{43} + k_{31}*k_{42} + k_{31}*k_{43} + L*k_{12}*k_{24} + L*k_{13}*k_{34} + L*k_{24}*k_{34} + L*k_{13}*k_{21} + L*k_{13}*k_{42} + \\
& L*k_{24}*k_{31} + L*k_{13}*k_{43} + L*k_{24}*k_{43} + L^2*k_{13}*k_{24})/6 + (k_{12}*k_{34}*k_{42})/2 + (k_{12}*k_{31}*k_{42})/2 + \\
& (k_{12}*k_{31}*k_{43})/2 + (k_{34}*k_{21}*k_{42})/2 + (k_{21}*k_{31}*k_{42})/2 + (k_{12}*k_{13}*k_{43})/2 + (L^2*k_{13}*k_{24}*k_{34})/2 + \\
& (L^2*k_{13}*k_{24}*k_{43})/2 + (L*k_{12}*k_{24}*k_{34})/2 + (L*k_{12}*k_{24}*k_{31})/2 + (L*k_{13}*k_{34}*k_{21})/2 + \\
& (L*k_{12}*k_{24}*k_{43})/2 + (L*k_{13}*k_{34}*k_{42})/2 + (L*k_{13}*k_{21}*k_{42})/2 + (L*k_{13}*k_{21}*k_{43})/2 + \\
& (L*k_{24}*k_{31}*k_{43})/2)^2 + ((k_{12}*k_{34})/3 + (k_{12}*k_{31})/3 + (k_{12}*k_{42})/3 + (k_{12}*k_{43})/3 + (k_{34}*k_{21})/3 + \\
& (k_{34}*k_{42})/3 + (k_{21}*k_{31})/3 + (k_{21}*k_{42})/3 + (k_{21}*k_{43})/3 + (k_{31}*k_{42})/3 + (k_{31}*k_{43})/3 - (k_{12} + k_{34} + \\
& k_{21} + k_{31} + k_{42} + k_{43} + L*k_{13} + L*k_{24})^{2/9} + (L*k_{12}*k_{24})/3 + (L*k_{13}*k_{34})/3 + (L*k_{24}*k_{34})/3 + \\
& (L*k_{13}*k_{21})/3 + (L*k_{13}*k_{42})/3 + (L*k_{24}*k_{31})/3 + (L*k_{13}*k_{43})/3 + (L*k_{24}*k_{43})/3 + (L^2*k_{13}*k_{24})/ \\
& 3)^3)^{(1/2)} - (k_{12}*k_{34}*k_{42})/2 - (k_{12}*k_{31}*k_{42})/2 - (k_{12}*k_{31}*k_{43})/2 - (k_{34}*k_{21}*k_{42})/2 - \\
& (k_{21}*k_{31}*k_{42})/2 - (k_{21}*k_{31}*k_{43})/2 - (L^2*k_{13}*k_{24}*k_{34})/2 - (L^2*k_{13}*k_{24}*k_{43})/2 - \\
& (L*k_{12}*k_{24}*k_{34})/2 - (L*k_{12}*k_{24}*k_{31})/2 - (L*k_{13}*k_{34}*k_{21})/2 - (L*k_{12}*k_{24}*k_{43})/2 - \\
& (L*k_{13}*k_{34}*k_{42})/2 - (L*k_{13}*k_{21}*k_{42})/2 - (L*k_{13}*k_{21}*k_{43})/2 - (L*k_{24}*k_{31}*k_{43})/2)^{(4/3)})
\end{aligned}$$

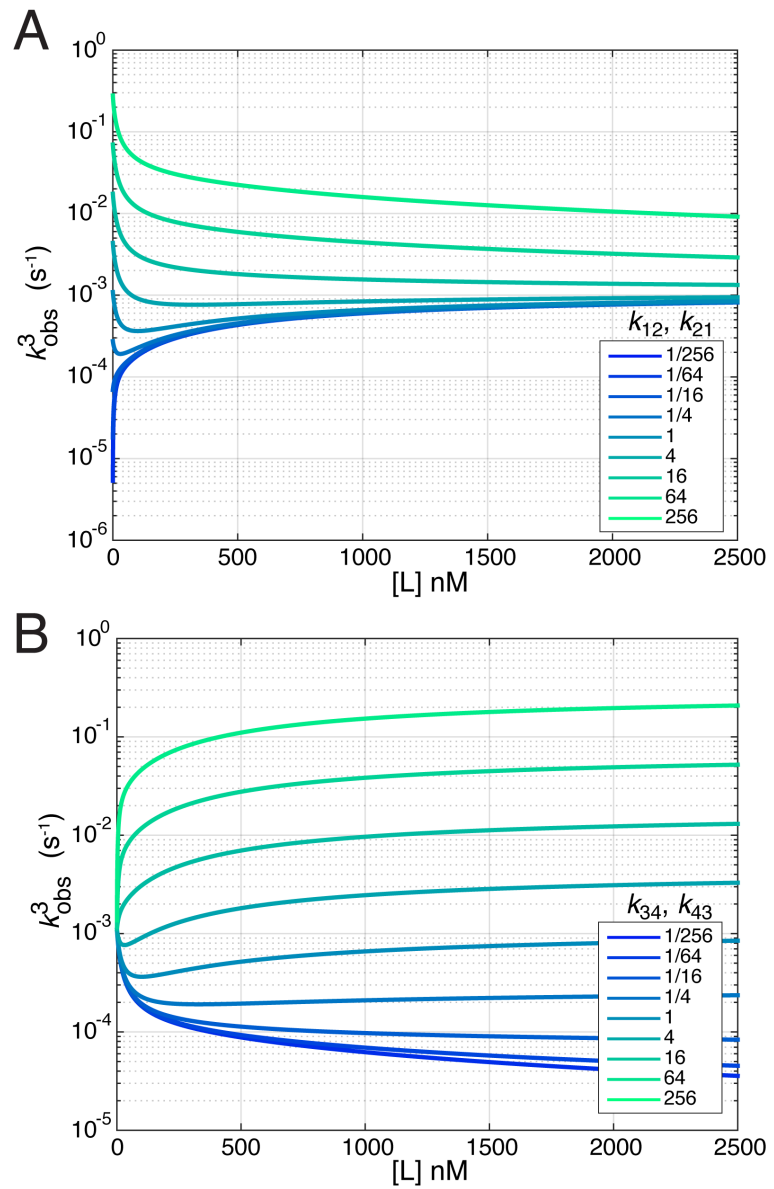
Supplemental Methods

Equilibrium fractional flux was calculated using the equations from Hammes et al. PNAS (2009). The fractional flux through the conformational selection pathway (F_{CS}) and the induced fit pathway (F_{IF}) are shown adapted to our nomenclature. Our calculations of flux were done under pseudo-first-order conditions, so our $[L]_{\text{free}} \approx [L]$.

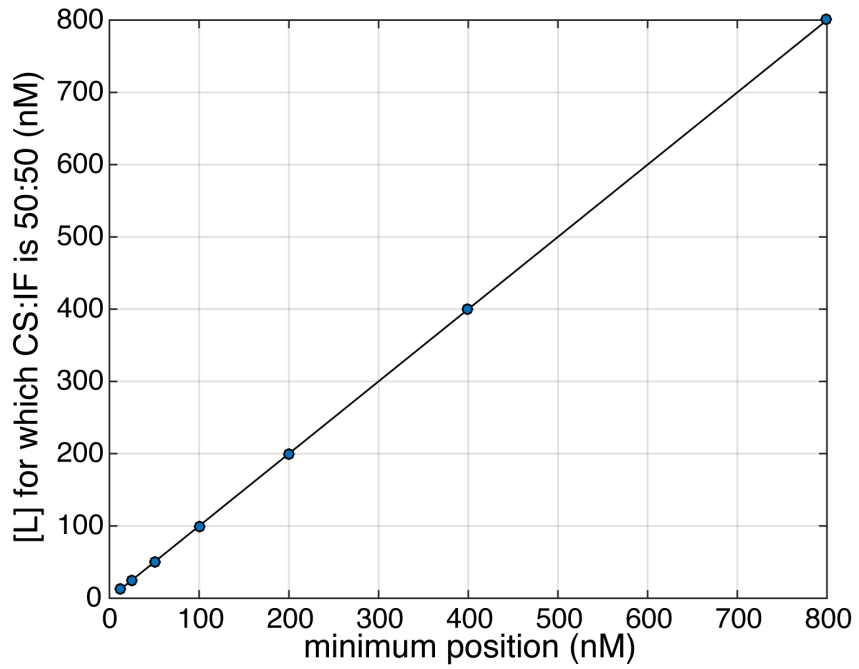
$$F_{CS} = \left(\frac{1}{k_{12}[A]} + \frac{1}{k_{24}[A^*][L]} \right)^{-1} \quad F_{IF} = \left(\frac{1}{k_{13}[A][L]} + \frac{1}{k_{34}[AL]} \right)^{-1}$$



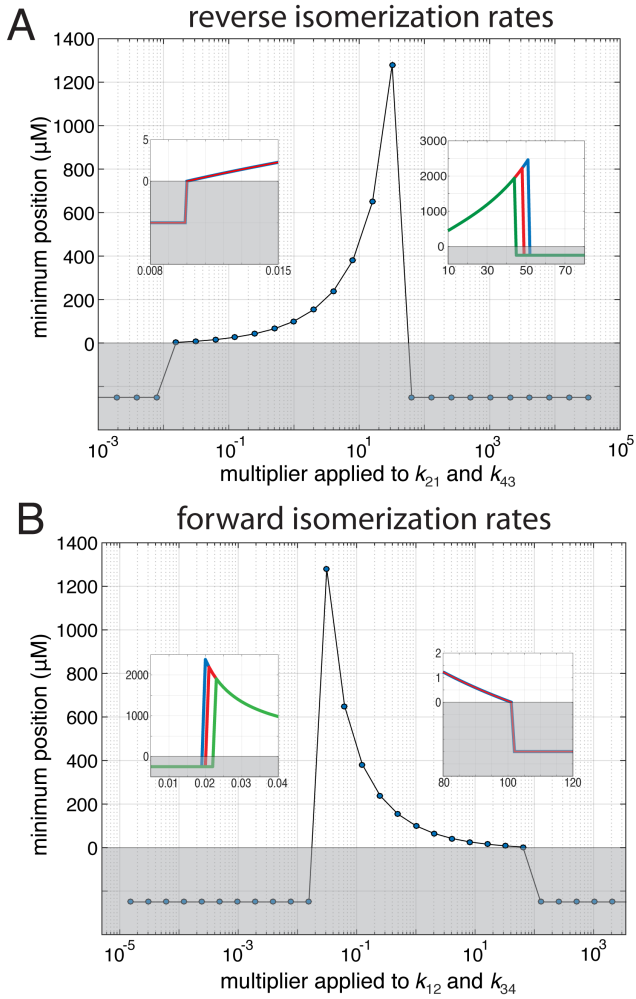
Supplemental Figure 1: Independence of curves on absolute rates of binding and dissociation of the individual complexes. Scaling the pairs of rates that describe the binding of L to **(A)** A (k_{13} and k_{31}) or **(B)** A* (k_{24} and k_{42}) do not affect the curves in the rapid equilibration regime. These titrations change the values of the rate pairs without changing the affinities.



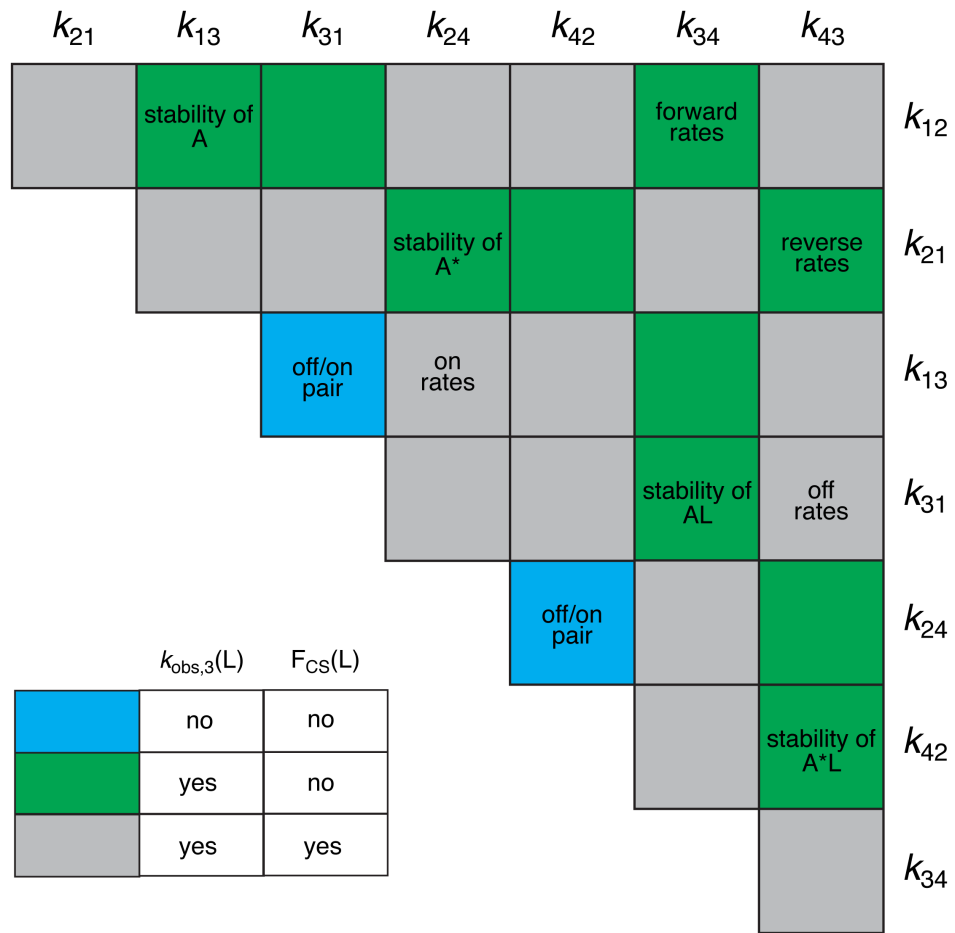
Supplemental Figure 2: Dependence of observed rate curves on the rates of isomerization.
The forward and reverse rates connecting **(A)** A and A* (k_{12} and k_{21}) or **(B)** AL and A*L (k_{34} and k_{43}) were multiplied by the values shown in the legend and the observed rate was plotted as a function of ligand concentration.



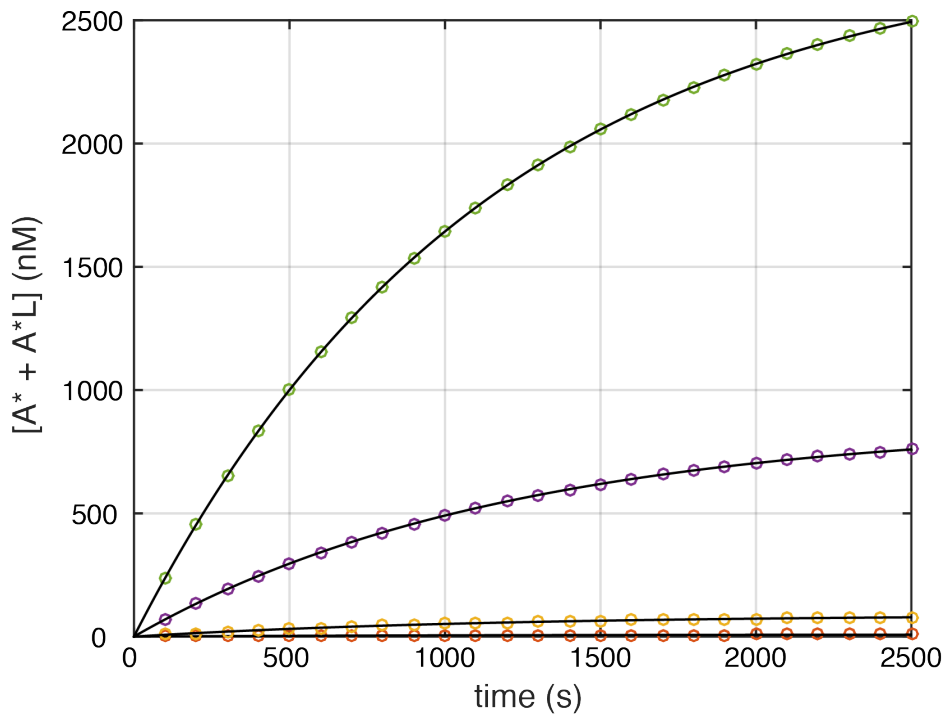
Supplemental Figure 3: Flux balance and the minimum observed rate occur at the same ligand concentration for the curves shown in Fig. 2 of the main text. The concentration at which 50% of the equilibrium flux occurs via each conformational selection and induced fit paths was calculated using the equations from Hammes and Oas {Hammes:2009}. The minimum position was determined by using a zero finding algorithm applied to the derivative of the third eigenvalue.



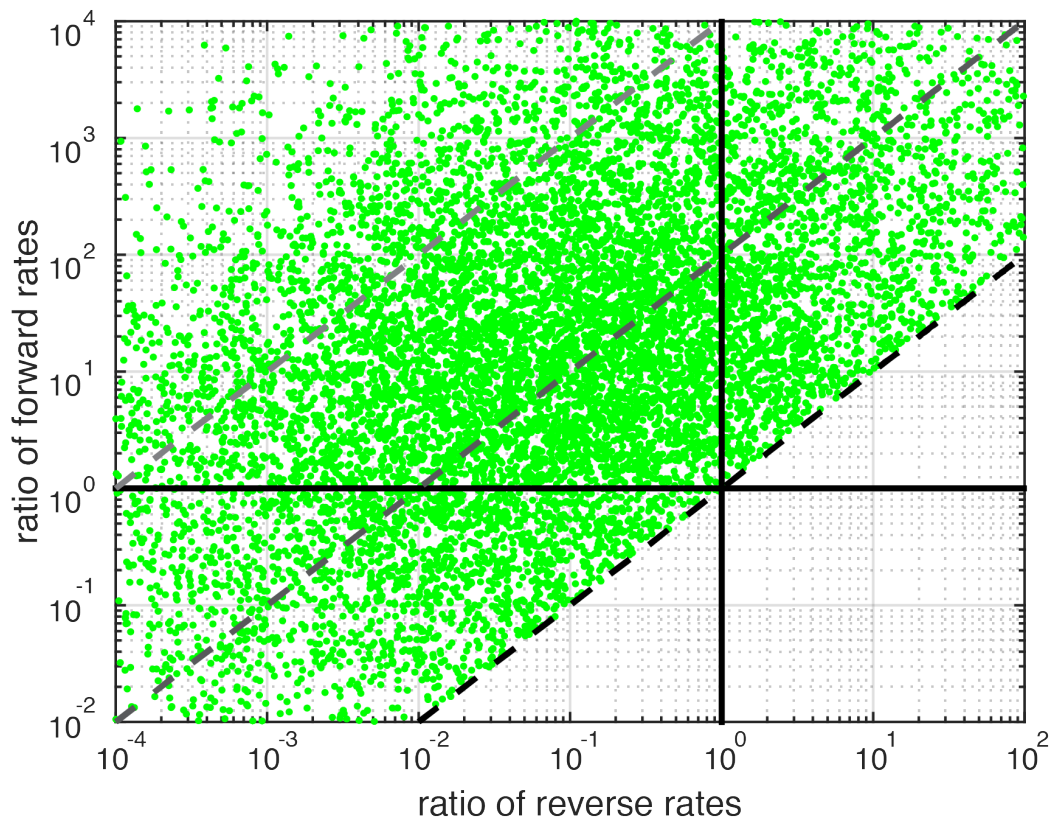
Supplemental Figure 4: Plots of zero positions for Fig. 3 of the main text. **(A)** The reverse rates in the bound (k_{43}) and un-bound (k_{21}) states were titrated together to conserve detailed balance. The ligand concentration at which a minimum is found in the third eigenvalue is plotted as a function of the applied multiplier. Negative values are used as a marker to indicate that no zero exists and are plotted in the shaded region. At high multipliers (fast reverse rates), the cutoff for the presence of a zero is arbitrary and depends on the maximum ligand concentration tested. The right inset shows three plots where the maximum concentration tested changes from 2000 μM (green), 2250 μM (red), and 2500 μM (blue). This is indicative that even curves that appear to only decrease, eventually increase at high enough ligand concentrations and stress the point that highest possible ligand concentrations should be always be tested in experimental systems. This does not occur at low multiplier values (slow reverse rates, left inset) as the curves overlap. **(B)** The same analysis is shown for titrations of the forward rates in both the bound (k_{34}) and un-bound (k_{12}) states. In this case, the cutoff for the presence of a minimum depends on the maximum concentration tested at low multipliers (slow rates, left inset), while the cutoff at high multipliers (fast forward rates, right inset) does not.



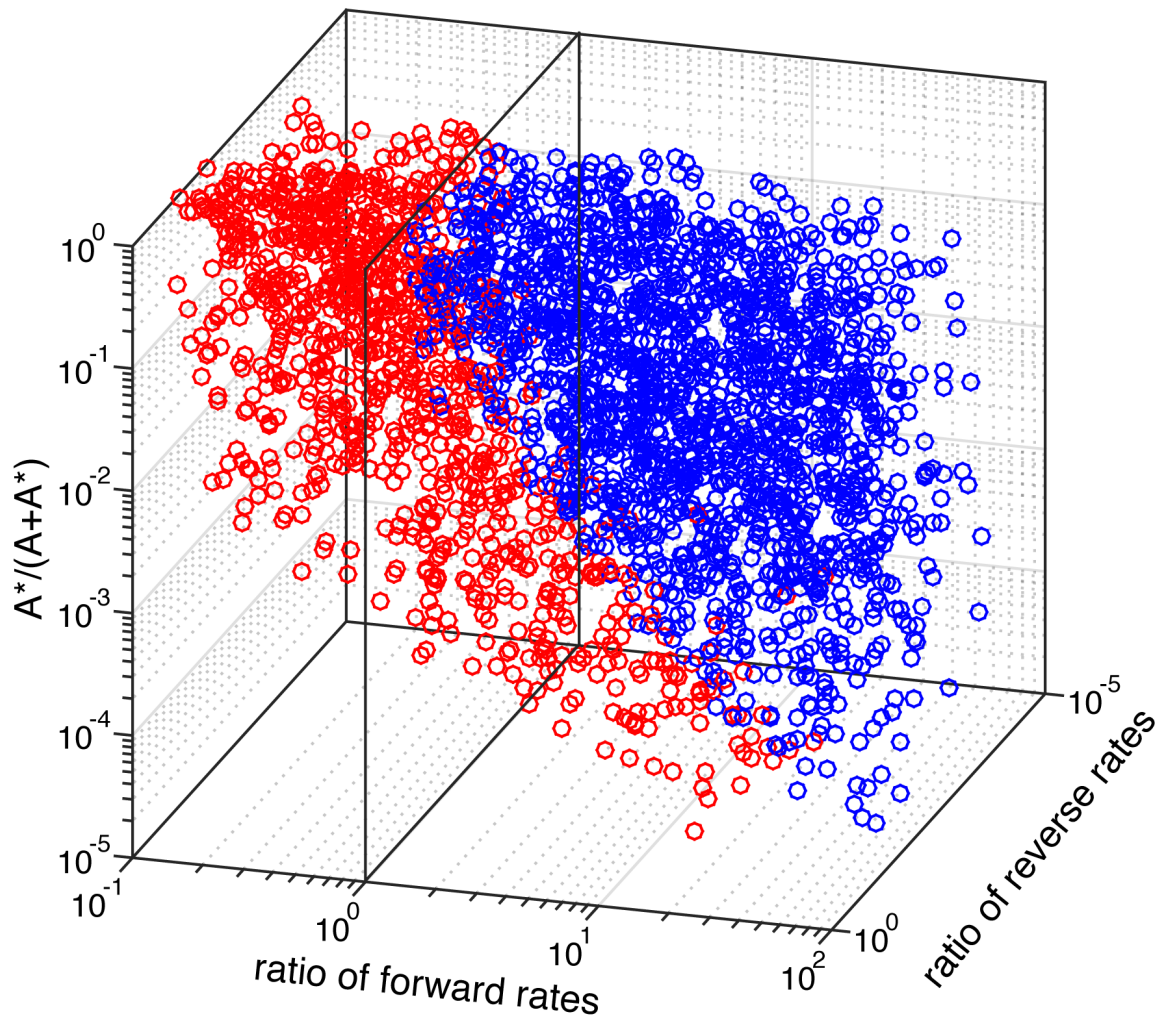
Supplemental Figure 5: Effect of scaling pairs of rates. The matrix displays each of the 28 possible pairs of rates within the 4-state thermodynamic cycle. Each square is color-coded by the effect that scaling that pair of rates has on both the ligand-dependence of the observed rate ($k_{\text{obs},3}$) and the equilibrium fractional amplitude (F_{CS}). Two rate pairs have not affect on either (blue), 10 rate pairs affect only the observed rate (green), and 16 rate pairs affect both (gray). The description of easily categorized rate pairs are shown within the appropriate squares.



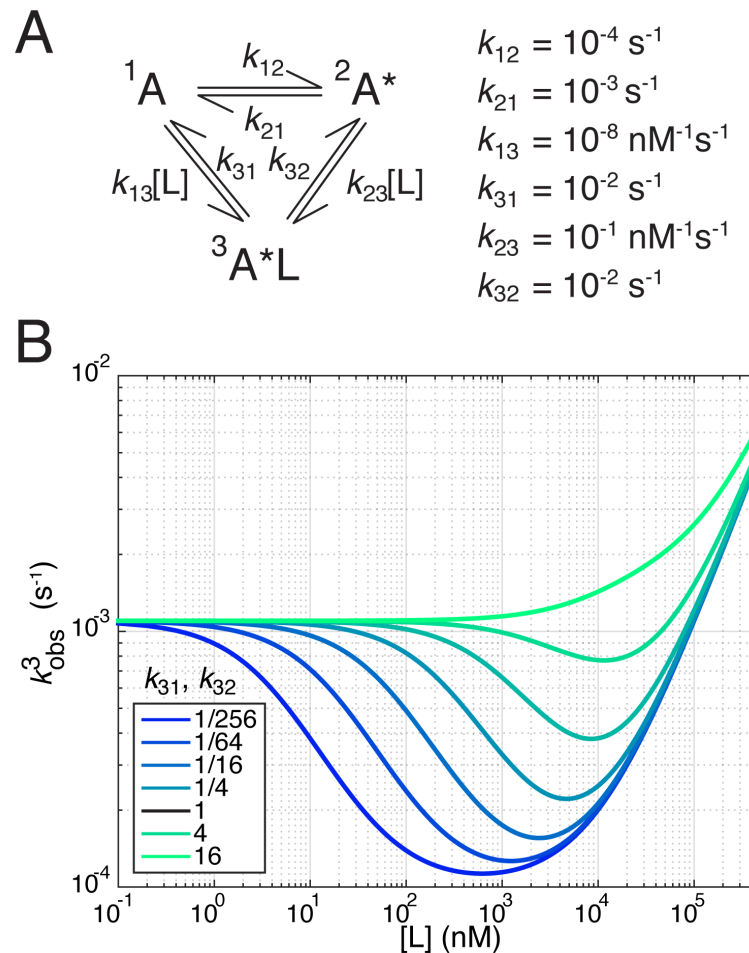
Supplemental Figure 6: Exponential fits of simulated non-pseudo-first order relaxation curves. The time-dependent evolution of the system was simulated by stepwise integration of the differential equations derived from the kinetic model. The observed rate of relaxation was estimated by fitting the time-dependence of the formation of total A^* (i.e. $A^* + A^*L$) with a single exponential. The examples shown above represent the simulation data for constant L (3000 nM) and four concentrations of A : 10 nM (red); 100 nM (yellow); 1000 nM (purple); and 5000 nM (green). The exponential fits used to estimate an observed rate for that condition are shown in black.



Supplemental Figure 7: Lack of non-monotonicity when rates of conformational exchange are more rapid than rates of ligand dissociation. Random sets of rates satisfying detailed balance were selected. Each rate was picked from a log-random distribution covering three orders of magnitude and centered on a rate set where the rates of conformational exchange are orders of magnitude faster than the off rates of binding. Specifically, $k_{12} = 10^5 * k_{42}$. Each rate set is represented as a single point on the graphs where the x-axis is the ratio of the reverse rates in the presence and absence of ligand (k_{21}/k_{43}) and the y-axis is the ratio of the forward rates in the presence and absence of ligand (k_{34}/k_{12}). The vertical and solid horizontal lines represent ratios of one for the reverse and forward rates respectively. The dashed diagonal lines represent contours of constant $\Delta\Delta G$ or degrees of stabilization of A^*L . In contrast to the sets shown in the main text, only monotonically increasing observed rates are observed (green) and both non-monotonic and monotonically decreasing trends are completely absent (blue and red points respectively in the main text Fig. 5).



Supplemental Figure 8: Three dimensional representation of rate space. Rate sets are plotted according to their fraction A^* in the absence of ligand (z-axis), ratio of reverse rates in the presence and absence of ligand (y-axis), and ratio of forward rates in the presence and absence of ligand (x-axis). Each point is an individual rate set and is color coded according to the trend in generates in the third observed rate. Sets that generate monotonically decreasing observed rates are red and those that display non-monotonicity are blue as in the main text.



Supplemental Figure 9: Minima in three-state cycle with conformational selection and a Koshland-like, one-step induced fit mechanism. (A) A three state thermodynamic cycle where the ligand (L) may bind to the two conformations A and A*. The binding of L to A* represents a conformational selection-type mechanism. The binding of L to A represents a Koshland-like induced fit mechanism where binding and conformational change occur simultaneously. This is in contrast to the induced fit mechanism described in the text where binding occurs first and increases the rate of conformational change.